Assessing the potential of amino acid ^{13}C patterns as a carbon source tracer in marine sediments: effects of algal growth conditions and sedimentary diagenesis

[1]T.Larsen [2]L. T.Bach [3]R.Salvatteci [3]Y. V.Wang [1]N.Andersen [4]M.Ventura [5]M. D.McCarthy

[1]Leibniz-Laboratory for Radiometric Dating and Stable Isotope Research, Christian-Albrechts-Universität zu Kiel, 24118 Kiel, Germany [2]Helmholtz-Zentrum für Ozeanforschung Kiel (GEOMAR), Düsternbrooker Weg 20, 24105 Kiel, Germany [3]Institute of Geoscience, Department of Geology, Kiel University, Ludewig-Meyn-Str. 10 24118 Kiel, Germany [4]Biogeodynamics and Biodiversity Group, Centre for Advanced Studies of Blanes (CEAB), Spanish Research Council (CSIC), 17300-Blanes, Catalonia, Spain [5]Ocean Sciences Department, UC Santa Cruz, Santa Cruz, CA 95064, USA

T. Larsen (natursyn@gmail.com)

Abstract

Burial of organic carbon in marine sediments has a profound influence in marine biogeochemical cycles, and provides a sink for greenhouse gases such as CO_2 and CH_4. However, tracing organic carbon from primary production sources as well as its transformations in the sediment record remains challenging. Here we examine a novel but growing tool for tracing the biosynthetic origin of amino acid carbon skeletons, based on naturally occurring stable carbon isotope patterns in individual amino acids ($\delta^{13}C_{AA}$). We focus on two important aspects for $\delta^{13}C_{AA}$ utility in sedimentary paleoarchives: first, the fidelity of source diagnostic of algal $\delta^{13}C_{AA}$ patterns across different oceanographic growth conditions; and second, the ability of $\delta^{13}C_{AA}$ patterns to record the degree of subsequent microbial amino acid synthesis after sedimentary burial. Using the marine diatom *Thalassiosira weissflogii*, we tested under controlled conditions how $\delta^{13}C_{AA}$ patterns respond to changing environmental conditions, including light, salinity, temperature, and pH. Our findings show that while differing oceanic growth conditions can change macromolecular cellular composition, $\delta^{13}C_{AA}$ isotopic patterns remain largely invariant. These results underscore that $\delta^{13}C_{AA}$ patterns should accurately record biosynthetic sources across widely disparate oceanographic conditions. We also explored how $\delta^{13}C_{AA}$ patterns change as a function of age, total nitrogen and organic carbon content after burial, in a marine sediment core from a coastal upwelling area off Peru. Based on the four most informative amino acids for distinguishing between diatom and bacterial sources (i.e. isoleucine, lysine, leucine and tyrosine), bacterial derived amino acids ranged from 10–15 % in the sediment layers from the last 5000 years, and up to 35 % during the last glacial period. The greater bacterial contributions in older sediments indicate that bacterial activity and amino acid resynthesis progressed, approximately as a function of sediment age, to a substantially larger degree than suggested by changes in total organic nitrogen and carbon content. It is uncertain if archaea may have contributed to sedimentary $\delta^{13}C_{AA}$ patterns we observe, and controlled culturing studies will be needed to investigate if $\delta^{13}C_{AA}$ patterns can differentiate bacterial from archeal sources. Further research efforts are also needed to understand how closely $\delta^{13}C_{AA}$ patterns derived from hydrolyzable amino acids represent total sedimenary proteineincous material, and more broadly sedimentary organic nitrogen. Overall, however, both our culturing and sediment studies suggest that $\delta^{13}C_{AA}$ patterns in sediments will represent a novel proxy for understanding both primary production sources, as well as the direct bacterial role in the ultimate preservation of sedimentary organic matter.

Introduction

Marine phytoplankton are responsible for nearly half the world's carbon net primary production (Field et al., 1998). While most of this production is rapidly decomposed or transferred to consumers within the shallow euphotic zone, a small fraction escapes from surface waters to the seafloor. While the fraction that eventually is buried in the sediment is small (on a global scale it has been estimated to be < 0.5 % (Hedges and Keil, 1995), marine sedimentary burial has a profound influence on the global carbon cycling over geological time scales (Burdige, 2007), representing the main preservation mechanism for reduced carbon in active biochemical cycles. Much progress in understanding the factors affecting organic matter preservation has been made in the last decades using trace metals and stable isotope ratios of oxygen, carbon and nitrogen in sediments (Cowie and Hedges, 1994; Henderson, 2002; Meyers, 2003; Tribovillard et al., 2006). However, the importance of different primary producers, as well as the role of microbes in sedimentary organic matter preservation remain key open questions, for which information must be derived from specific organic tracers.

Amino acids are one of the most studied biochemical classes in organic geochemistry, because they are major constituents of phytoplankton (Nguyen and Harvey, 1997; Wakeham et al., 1997), and also sensitive tracers for diagenetic processes (Dauwe et al., 1999; Lomstein et al., 2006). In the open ocean, the majority of organic carbon in both plankton and sinking particular organic matter (POM) is in the form of amino acids (Lee et al., 2000; Hedges et al., 2001). However, because amino acids are also more labile than bulk organic matter (Cowie and Hedges, 1994), degradation also changes the composition of protein amino acids in particles and sediments, in part by introducing new bacterial derived biosynthate (Grutters et al., 2002; Lomstein et al., 2006). This means that amino acids preserved in sediments represent a mixture of those derived from original autotrophic sources, as well as those that have been subject to subsequent diagenetic alteration. In degraded organic matter mixtures (including sediments) amino acid origins can be complex, with the potential for selective degradation or de novo synthesis via heterotrophic bacterial metabolism (McCarthy et al., 2007).

Tracing original autotrophic sources has long been one of the most important biomarker applications in many areas of organic geochemistry. Recent research has demonstrated that naturally occurring $\delta^{13}C$ variations among amino acids (i.e. $\delta^{13}C_{AA}$ patterns), can be directly linked to biosynthetic origin (Larsen et al., 2009, 2013). These $\delta^{13}C_{AA}$ patterns, or fingerprints, are generated during biosynthesis, and can potentially be used as high fidelity markers or fingerprints of algal, bacterial, fungal and plant origins of amino acids, and by extension a large fraction of total organic matter. In contrast to bulk isotope approaches, where often uncertain "baseline" values for a given environment are essential for correctly inferring provenance of carbon, recent results have suggested that $\delta^{13}C_{AA}$ fingerprints are largely independent of variation in baseline isotope values. For example, Larsen et al. (2013) found that variations in bulk $\delta^{13}C$ values were between five and ten times greater than variation in $\delta^{13}C$ values between individual amino acids for seagrass (*Posidonia oceanica*) and giant kelp (*Macrocystis pyrifera*), collected at different times or location in the natural environment. These findings suggest that sedimentary $\delta^{13}C_{AA}$ patterns may lead to a new approach to assess major primary or secondary production contributions to sediments. However, controlled physiological studies have never been conducted to test whether $\delta^{13}C_{AA}$ patterns from algae remain constant under varying environmental conditions.

A second key issue is the degree to which $\delta^{13}C_{AA}$ patterns preserved in sediments reflect original exported production, as opposed to secondary bacterial production occurring after deposition. Understanding the balance between major sources of preserved organic carbon is central to understanding how changes in productivity of marine ecosystems may ultimately affect global carbon cycles. Highly productive coastal ecosystems, such as the Peruvian upwelling area, have a particularly large impact on global carbon sequestration, because of the high fluxes and preservation of particulate organic matter. Particulate organic matter in such systems are often deposited under oxygen-deficient to anoxic conditions, allowing a much larger proportion of primary production to be ultimately preserved than is typical of open ocean regions (Hartnett et al., 1998). Sediments from the Peruvian upwelling region represent one endmember of sedimentary depositional conditions, and therefore an ideal first environment in which to examine the extent to which $\delta^{13}C_{AA}$ patterns reflect original phytoplankton sources, vs. subsequent bacteria resynthesis.

Here we report for the first time experiments that directly explore these two main issues for $\delta^{13}C_{AA}$ sedimentary applications, focusing on understanding both $\delta^{13}C_{AA}$ source patterns across large variation in growth conditions, and then quantifying evidence for bacterial influence in ultimate sedimentary preservation. To address the question of whether $\delta^{13}C_{AA}$ patterns of phytoplankton remain constant under varying environmental conditions, we cultured *Thalassiosira weissflogii* under controlled conditions. *Thalassiosira weissflogii* is an abundant, nitrate-storing, bloom-forming diatom with high phenotypic plasticity, i.e. ability to change macromolecular composition (Diekmann et al., 2009; Kamp et al., 2013). Diatoms are a diverse and ecologically important group contributing up to 40 % of the oceans primary production (Nelson et al., 1995). To investigate how $\delta^{13}C_{AA}$ patterns are transformed during early diagenesis, we analyzed a 45 000 year old (45 kyr) sediment core collected off the Peru margin, in an area characterized by high sedimentation rates and low oxygen. We specifically focused on using $\delta^{13}C_{AA}$ patterns to directly estimate change in relative proportions of algal vs. heterotrophic microbial amino acids with age.

1 Material and methods

1.1 Culture experiment

The marine diatom *Thalassiosira weissflogii* Grunow (strain CCMP 1010) was cultured in sterile filtered North Sea water (Schleswig-Holstein, Germany) or Baltic Sea water (Schleswig-Holstein, Germany). The medium was enriched with f/4 concentrations of macro- and micronutrients (nitrate, phosphate, silicic acid, trace metal mixture, vitamin mixture as described by Guillard and Ryther (1962). All experiments were performed in sterile 2.1 L Schott Duran glass bottles. These bottles were made of borosilicate glass (filters UV radiation < 310 nm) except for the quartz glass bottles (pure silica without UV radiation filter) used in the UV experiment (Table 1). The cultures were either incubated in climate chambers with 400–700 nm radiation or 10 cm below water level at low tide in Kiel Fjord in May 2011. Water temperature and light irradiance data were obtained from the weather station maintained by the GEOMAR institute in Kiel, Germany. Growth conditions for the various treatments, i.e. salinity, pH, temperature and irradiance are given in Table 1. pH values were measured with separate glass and reference electrodes (Metrohm) and calculated with Eq. (3) from DOE 2007 Chapter 6b in Dickson et al.

(2007) and corrected as described in Bach et al. (2012). Cultures were inoculated with densities of 20 cells mL^{-1}. Cell densities and equivalent spherical diameters were determined with a Coulter Counter (Beckman Coulter) at the beginning and the end of the experiment, respectively. Growth rates and cell diameters are reported in Table 2. When incubations ended, cells were filtered on 47 mm diameter, 5 m mesh size Nucleopore Track-Etch Membrane filters (Whatman) and frozen at -18 C immediately after filtration.

1.2 Sediment samples

Sediment samples were retrieved from a 14.97 m long piston core (M772-003-2) collected on 2008 by the Meteor cruise at 271 m water depth within the main upwelling area off Peru (156.21ºS, 7541.28ºW). At the time of sampling, the O_2 concentration at the seafloor was 1.1 $g\ L^{-1}$, i.e. nearly anoxic conditions. We obtained count and species assemblage of diatoms from Mollier-Vogel (2012). The site can according to the algal abundance and nitrogen content be characterized as highly productive; for the sediment layers analyzed in this study, the percentage of algal upwelling species was larger than 60 % (Table 3).

The age for core M772-003-2 is based on 16 radiocarbon dates measured at the AMS facility of the Leibniz-Laboratory for Radiometric Dating and Isotope Research at Kiel University (Grootes et al., 2004). Radiocarbon measurements were carried out on organic matter instead of foraminifera due to extensive periods of dissolution of foraminifera in Peruvian marine sediments (e.g., Makou et al., 2010). Prior to determination of organic matter content, sediment samples were pre-treated with an acid-alkali-acid cleaning with HCl and NaOH (Grootes et al., 2004). For the age model and sedimentation rates see Schönfeld et al. (2014) and Mollier-Vogel (2012). In brief, the radiocarbon dates were performed on the humic acid fraction, which contains organic matter mainly from marine origin. Radiocarbon dates were calibrated for the global ocean reservoir age using the MARINE09 calibration curve (Reimer et al., 2009). Additionally, the radiocarbon dates were calibrated for regional reservoir effect (ΔR) using a value of 511 ± 278 years (Ortlieb et al., 2011). The age model of the core is based on linearly interpolated ages between the calibrated radiocarbon ages. A temporal gap of 20.000 years (from 17.4 to 37.8 kyr BP) was found at 10.3 m depth, which is a common feature on sediments retrieved from the Peruvian continental shelf (Skilbeck and Fink, 2006; Salvatteci et al., 2014).

1.3 Stable isotope analyses

Both diatom and bulk sediment samples were freeze dried prior to isotopic analysis. To prepare aliquots for derivatization of amino acids, we used 3–4 mg of diatoms and 100–150 mg of sediments. The samples were transferred to Pyrex culture tubes (13×100 mm), flushed with N_2 gas, sealed, and hydrolysed in 1 mL 6N HCl at 110°C for 20 h. After hydrolysis, lipophilic compounds were removed by vortexing with 2 mL *n*-hexane/DCM (6 : 5, v / v) for 30 s. The aqueous phase was subsequently transferred through disposable glass pipettes lined with glass wool into 4 mL dram vials. Samples were evaporated to dryness under a stream of N_2 gas for 30 min at 110 C before being stored at -18°C. Before derivatization, sediment samples were purified with Dowex 50WX8 cation exchange 100–200 mesh resin according to Amelung and Zhang (2001) and He et al. (2011). The purification removes interferring organic substances with the result that co-elution of unwanted compounds are minimized during chromatographic separation (see Fig. S1 in the Supplement for a sediment sample GC trace). The purification also ensures that isotope

fractionation associated with acetylation and methylation of amino acids are comparable across sample types. Since it was unknown whether the purification process would affect $\delta^{13}C$ values of amino acids, we performed a test on freeze-dried yeast samples and a mixture of amino acid standards, respectively. For both sample types, asparagine/aspartate (Asx) was significantly enriched by approximately 1.5 ‰ compared to the controls (see Fig. S2). For the remaining amino acids, we found no consistent isotope effects of purification indicating that $\delta^{13}C_{AA}$ alues of purified and non-purified samples are comparable except for Asx. The derivatization procedure, which serves to convert the non-volatile amino acids to a volatile derivatives, was modified from Corr et al. (2007) as described by Larsen et al. (2013). Briefly, the dried samples were methylated with acidified methanol and subsequently acetylated with a mixture of acetic anhydride, triethylamine, and acetone, forming N-acetyl methyl ester derivatives. As a precautionary measure to reduce the oxidation of amino acids, we flushed and sealed reaction vials with N_2 gas prior to methylation and acetylation. Another modification from Corr et al. (2007) was that ice baths in that protocol were substituted here with solid aluminum blocks at room temperature. We used known $\delta^{13}C$ values of pure amino acids prepared and analyzed under the same conditions as the samples to calculate correction factors specific to each amino acid to account for carbon addition and fractionation during derivatization. The derivatized amino acids were dissolved ethyl acetate and stored at 18°C until required for analysis.

Amino acid $\delta^{13}C_{AA}$ values were obtained from Leibniz-Laboratory for Radiometric Dating and Stable Isotope Research in Kiel. We injected the amino acid derivatives into a PTV injector held at 250 C for 4 min before GC separation on an Agilent 6890N GC. Diatom samples were separated on an Rtx-200 column (60 m $\times$ 0.32 mm $\times$ 0.25 µm) and sediment samples on a Thermo TraceGOLD TG-200MS GC column (60 m $\times$ 0.32 mm $\times$ 0.25 µm). For both GC columns, the oven temperature of the GC was started at 50°C and heated at 15°C min^{-1} to 140°C, followed by 3°C min^{-1} to 152°C and held for 4 min, then 10°C min^{-1} to 245°C and held for 10 min, and finally 5°C min^{-1} to 290°C and held for 5 min. The GC was connected with a MAT 253 isotope ratio mass spectrometer (IRMS) via a GC-III combustion (C) interface (Thermo-Finnigan Corporation). We obtained consistently good chromatography for alanine (Ala), valine (Val), leucine (Leu), isoleucine (Ile), Asx, threonine (Thr), methionine (Met), glutamine/glutamate (Glx), phenylalanine (Phe), tyrosine (Tyr), lysine (Lys), and arginine (Arg) with the exception that Asx and Thr partially coeluted on the Rtx-200 column. Serine (Ser) and proline (Pro) coeluted on both columns. The average reproducibility for the norleucine internal standard was ±0.4 ‰ (*n*=3 for each sample), and the reproducibility of amino acid standards ranged from ±0.1 ‰ for Phe to ±0.6 ‰ for Thr (*n*=3). See Tables S1 and S2 in the Supplement for $\delta^{13}C_{AA}$ values of diatom and sediment samples, respectively.

Amino acid molar composition was determined with the derivative samples used for $\delta^{13}C_{AA}$ analysis. The amino acids were separated on an Rxi-35SIL MS column (30 m $\times$ 0.32 mm $\times$ 0.25 m) with an Agilent 6890N GC with a flame ionization detector. With this column we obtained good chromatography for Ala, Asx, Glx, Gly, Ser, Tyr, Arg, Ile, Leu, Lys, Met, Phe, Thr, and Val. For quantification, we used internal references consisting of pure amino acids (Alfa Aesar, Karlsruhe, Germany). For comparison between molar composition and isotope values, amino acids were subdivided into the following biosynthetic families: Pyruvate (Ala, Leu, Val), Oxaloacetate (Asx, Ile, Lys, Met, Thr), α-keoglutarate (Arg, Glx), 3-phosphoglycerate (Gly, Ser), and Shikimate (Phe, Tyr).

Bulk ^{13}C and ^{15}N values, and the elemental composition of carbon and nitrogen (% C and % N respectively, expressed as percentage by mass) of the diatom samples were determined at the

UC Davis Stable Isotope Facility using a PDZ Europa ANCA-GSL elemental analyzer interfaced to a PDZ Europa 20-20 isotope ratio mass spectrometer (Sercon Ltd., Cheshire, UK). The dry weight of the samples ranged between 1.5 and 2.5 mg. During analysis, samples were interspersed with several replicates of at least three different laboratory standards. These laboratory standards, which were selected to be compositionally similar to the samples being analyzed, had previously been calibrated against NIST Standard Reference Materials (IAEA-N1, IAEA-N2, IAEA-N3, USGS-40, and USGS-41). A sample's preliminary isotope ratio was measured relative to reference gases analyzed with each sample. These preliminary values were finalized by correcting the values for the entire batch based on the known values of the included laboratory standards. The long term standard deviation is 0.2 ‰ for $\delta^{13}C$ and 0.3 ‰ for $\delta^{15}N$. See Mollier-Vogel (2012) for $\delta^{15}N$ and total nitrogen content determination of the sediment samples. Briefly, the sediment samples were measured at the University of Bordeaux 1 (EPOC, UMR CNRS 5805, France), on 5 to 60 mg of homogenized and freeze-dried bulk sediment. Samples were encapsulated in tin cups and then injected into a Carlo-Erba CN analyser 2500 coupled directly to a Micromass-Isoprime mass spectrometer. $\delta^{13}C$

1.4 Calculations and statistical analyses

All statistical analyses were performed in R version 3.0.2 (R-Development-Core-Team, 2014) using the RStudio interface version 0.98.493. Prior to testing differences between diatom treatments with analysis of variance (ANOVA) and Tukey HSD post-hoc tests, $\delta^{13}C_{AA}$ values were normalized to the mean of all the AAs ($\delta^{13}C_{AAnor}$; Thr, Met, Arg were excluded due to their large treatment variations) and tested for univariate normality by visually checking whether there were departures from normality on *Q-Q* plots. We denoted $\delta^{13}C_{AA}$ values that were not normalized to the mean as absolute values ($\delta^{13}C_{AAabs}$). To examine combinations of independent variables (i.e. $\delta^{13}C_{AA}$ values) that best explained differences between the categorical variables and to construct models for predicting membership of unknown samples, we performed linear discriminant function analysis (LDA, R package MASS) (Venables and Ripley, 2002) with $\delta^{13}C_{AA}$ values. To test the null hypothesis that there was no difference in classification between the groups we applied Pillai's trace (MANOVA). To identify significant correlation between sediment $\delta^{13}C_{AA}$ values and explanatory variables we performed multiple scatterplot matrices. For model simplification of multiple linear regression we performed a penalized log likelihood. We estimated the proportion of amino acid biosynthetic origins using the Bayesian mixing model FRUITS ver 2.0 (Fernandes et al., 2014b). We also performed principle component analysis (PCA, R package vegan) with $\delta^{13}C_{AAnor}$ values and amino acid molar composition.

To estimate the changes of molar composition of protein amino acids as a result of diagenesis, we also determined the degradation index (DI) of sediment amino acids according to Dauwe and Middelburg (1998);

$$\mathrm{DI} = \sum_i [(\mathrm{var}_i - \mathrm{AVGvar}_i)/\mathrm{STDvar}_i] \times \mathrm{fac.coef}_i \quad (1)$$

where var_i is the nonstandardized mole percentage of amino acid i in our dataset, AVGvar_i and STDvar_i are the mean and standard deviation, and $\mathrm{fac.coef}_i$ is the first PCA factor coefficient for amino acid i. The factor coefficients, averages, and standard deviations were taken from Dauwe et al. (1999).

2 Results

2.1 Culture experiment with diatoms

The range in $\delta^{13}C$ values between the most depleted and most enriched treatments was 11 in part owing to differences in carbonate chemistry speciation (Tables 1 and 2). When omitting the low salinity and high pH treatments, which both had markedly different buffering capacity, bulk $\delta^{13}C$ values were linearly correlated with cell densities ($p< 0.001$, R^2=0.732) reflecting that CO_2 as a source for carbon fixation became limiting as cell densities became high. Temperature was by far the most important parameter controlling growth rates ($p< 0.001$, R^2=0.877).

The $\delta^{13}C_{AA}$ patterns of *T. weissflogii* across all 10 treatments were quite similar in spite of the large span in $\delta^{13}C$ baseline (i.e., bulk $\delta^{13}C$ values; Fig. 1). The mean range in $\delta^{13}C_{AAnor}$ values for the 11 AAs (Thr omitted due to large variability between replicates) was 1.4 $\pm$ 0.7 ‰ compared to 6.1 $\pm$ 0.9 ‰ for $\delta^{13}C_{AAabs}$ values (Fig. 2). The maximum range was 2.6 $\pm$ 0.9 ‰ for $\delta^{13}C_{AAnor}$ values and 11.1 $\pm$ 0.8 ‰ for $\delta^{13}C_{AAabs}$ values. Thus, both $\delta^{13}C_{bulk}$ and $\delta^{13}C_{AAabs}$ values were about four times greater than $\delta^{13}C_{AAnor}$ values. The amino acids with the smallest $\delta^{13}C_{AAnor}$ values (< 2) were Met, Leu, Phe, Glx and Ile. The amino acids with the least variability tended to be the ones with long and complicated biosynthetic pathways, i.e. the amino acids considered essential for animals. However, certain essential amino acids such as Lys and Val had greater $\delta^{13}C_{AAnor}$ values than non-essential amino acids such as Glx and Ala.

We also plotted the offsets in $\delta^{13}C_{AAnor}$ values between the control and the remaining treatments (Fig. 3). Almost all offset values were within 1 , except for amino acids with high variability between replicates, such as Thr, Asx and Arg. We found the largest offsets relative to the control among treatments with high cell densities (27° C, low salinity, 18° C; Table 2). Finally, to confirm that $\delta^{13}C_{AA}$ patterns of *T. weissflogii* would remain diagnostic of their autotrophic source, regardless of these relatively small changes in $\delta^{13}C_{AAnor}$ values associated with different growth conditions, we compared our *T. weissflogii* data with a published datasets for two other main marine taxa, seagrass and kelp, collected from a range of different natural marine habitats (Larsen et al., 2013). The PCA showed that the three taxa clustered apart, and almost all of the amino acids were important for explaining variation in the multivariate data set (Fig. 4). This result suggests that the magnitude of change in $\delta^{13}C_{AA}$ patterns associated with changing growth conditions does not affect the basic diagnostic ability of amino acids to track phylogenetic carbon source.

We investigated how growth conditions affected stoichiometric composition of the diatom cells (Table 2). The results show that amino acid molar composition correlated to both cell size and to C : N ratio. The C : N ratios broadly correlated to amino acid composition across biosynthetic families; proportions of Gly, Tyr, Lys, Met and Arg increased significantly with higher C : N ratios (R^2 values ranged from 0.657 to 0.846, $P < 0.001$), while the proportions of Leu, Asx, Ile, Val, Glx and Phe decreased (R^2 values ranged from 0.661 to 0.760, $P < 0.001$). We also found similar relationships between cell size and amino acid composition, presumably owing to the positive correlation between C : N ratios and cell size ($P < 0.001$, $R^2 = 0.831$).

To explore the possibility that variations in $\delta^{13}C_{AA}$ patterns were connected with the stoichiometric composition of the cells, we correlated $\delta^{13}C_{AAnor}$ to the relative molar composition of amino acid biosynthetic families and carbon (% C), nitrogen (% N) and the ratio of both elements (C : N). For all amino acids except Ala, Tyr and Phe, correlations between $\delta^{13}C_{AAnor}$ values

and C : N ratios were weak ($R^2 \leq 0.37$), and in most cases insignificant ($P > 0.05$). In the pyruvate family, Ala was the amino acid with the strongest correlations to the 3-PGA and Shikimate families, and C : N ratios, respectively, with R^2 values ranging from 0.569 to 0.650 ($P < 0.001$). While $\delta^{13}C_{AAnor}$ values of Ala became more enriched with increasing proportions of Pyruvate amino acids, the relationship was opposite for the 3-PGA and Shikimate families, and also for C : N ratios. Correlations between Ala and the oxalo and a-ketoglutarate families were non-significant ($P > 0.05$). Finally, the trends for Tyr and Phe in the Shikimate families were the opposite of those observed for Ala. The linear correlations between Tyr or Phe to biosynthetic families and C : N ratios were significant, but much weaker ($P < 0.001$, $R^2 \leq 0.462$) compared to Ala. We did not find that any of the remaining environmental and physiological parameters correlated tightly with $\delta^{13}C_{AAnor}$ values.

2.2 Sediment samples

To investigate the degree of bacterial-like $\delta^{13}C_{AA}$ patterns in the sediment samples, we first performed LDA to identify which set of amino acids that best would distinguish between diatoms and bacteria, using a training dataset based on laboratory cultured diatoms and bacteria by Larsen et al. (2013). In the training dataset, we also included the diatoms *Stauroneis constricta* and *T. weissflogii* cultured specifically for this study under conditions similar to the control treatment described previously (Table 1). To avoid single-species bias in the training dataset, we did not include the 28 *T. weissflogii* samples from the culture experiment. The LDA results, which was based on $\delta^{13}C$ values of nine amino acids, showed that bacteria and diatom each have distinct $\delta^{13}C_{AA}$ patterns with Ile, Lys, Leu and Tyr providing the best discrimination between groups according to the coefficient values in Fig. 5. Most sediment samples classified with 100 % probability as either bacteria or diatoms via the LDA; however, the linear discriminant scores were generally intermediate between bacteria and diatoms indicating that the original primary production sources were reworked by bacteria. Since LDA is intrinsically non-quantitative, a classification method indicating probable associations, it is poorly suited for estimating the proportion of bacterial vs. diatom derived amino acids. For this reason we explored two other statistical approaches.

The first statistical approach for estimating the relative proportion of bacteria was based on a Bayesian mixing model FRUITS using $\delta^{13}C_{AAnor}$ values. We selected Leu, Lys, Ile and Tyr because they have the largest discriminant scores for separating diatoms and sediments (Fig. 5). Based on the Bayesian model, the sedimentary contribution of bacterial-derived amino acids ranged from 10–15 % in the upper layers, and to up to 35 % in deeper layers, with standard deviation values ranging between 8 and 20 % (Fig. 6, for more information see Fig. S1 and Table S3). The larger bacterial fractions in deeper layers indicate that accumulation of bacterial biosynthate continued to increase as a function of age throughout this core.

In the second statistical approach, we used multiple linear regression analyses correlating $\delta^{13}C$ differences between pairs of amino acids with other sediment parameters. By analyzing all possible pairwise combinations of sediment $\delta^{13}C_{AA}$ values, we found that Leu relative to Lys, Ile and Tyr were highly significant as a function of sediment age. For the $\delta^{13}C_{Lys\text{-}Leu}$ combination, age, % organic C, and algal abundance explained 97.3 % of the variation (Table 4). The offsets between $\delta^{13}C_{Lys}$ and $\delta^{13}C_{Leu}$ became smaller with age ($P < 0.001$, $R^2 = 0.572$, in contrast to organic C content ($P < 0.05$, $R^2 = 0.525$). Algal abundance was not significant as a single explanatory variable ($P > 0.05$). The trends in $\delta^{13}C_{Lys\text{-}Leu}$ values as a function of age was similar to that of the bacterial amino

365 acid fraction calculated with FRUITS (Fig. 6). We also compared $\delta^{13}C_{Lys\text{-}Leu}$ values with another
366 diagenetic parameter, DI (Table 3), and found that the correlation between these two parameters
367 was weak but significant with an R^2 value of 0.40 ($P \leq 0.05$) in contrast to the correlation between.
368 age and DI ($P > 0.05$). In regard to the remaining pairwise combinations with Leu, $\delta^{13}C_{Ile\text{-}Leu}$, age
369 and % organic C explained 73.2 % of the variation, and $\delta^{13}C_{Tyr\text{-}Leu}$, age and % organic C explained
370 64.8 % of the variation (Table 4). None of the other sediment parameters were as important as
371 age: $\delta^{13}C_{Glx\text{-}Phe}$ as a function of %N had an R-squared value of 0.542, and $\delta^{13}C_{Thr\text{-}Ala}$ as a function of
372 algal abundance had an R-squared value of 0.744. DI values did not correlate with any of the
373 pairwise combination of sediment $\delta^{13}C_{AA}$ values.
374
375 # 3 Discussion
376
377 ## 3.1 Sensitivity of $\delta^{13}C_{AA}$ patterns to algal growth conditions
378
379 To investigate whether $\delta^{13}C_{AA}$ patterns remain diagnostic of source across different growth
380 conditions, we exposed the cosmopolitan diatom *T. weissflogii* to different treatments in the
381 laboratory. We found that $\delta^{13}C_{AA}$ patterns of *T. weissflogii* across all 10 different treatments
382 remained consistent (Fig. 1), and so retained the ability to trace primary producer carbon source.
383 This finding was underscored by our comparison to literature data from two other dominant
384 marine taxa, seagrass and kelp, collected from different natural habitats. The range in baseline
385 $\delta^{13}C$ values (i.e., bulk $\delta^{13}C$) of the diatoms was about 11 , compared to about 2–3 for $\delta^{13}C_{AAnor}$
386 values. No specific treatment induced larger than average variation in $\delta^{13}C_{AA}$ patterns. In terms of
387 macromolecular composition, the finding that C : N ratios varied two-fold across treatments
388 indicates that, as has been observed previously, lipid to protein ratios vary widely with growth
389 conditions (Tsuzuki et al., 1990; Dohler and Biermann, 1994; Rousch et al., 2003; Torstensson et
390 al., 2013). Changes in amino acid molar composition were relatively modest in comparison; the
391 largest differences in relative composition were in the pyruvate and 3-PGA families, with 30–40 %
392 offset between treatments, and the smallest in the oxaloacetate family with < 10 % offset.
393 Overall, our findings indicate that while differing oceanic growth conditions may change
394 macromolecular composition, $\delta^{13}C_{AA}$ isotopic patterns remain largely invariant. This conclusion is
395 strongly supported by previously published results for both giant kelp and seagrass (Larsen et al.,
396 2013), and is also consistent with the results from two recent natural food-web studies (Arthur et
397 al., 2014; Vokhshoori et al., 2014). Together, these results represent the first controlled
398 experimental confirmation that $\delta^{13}C_{AA}$ patterns represent reliable carbon source tracers for
399 primary production, irrespective of growth environment.
400 More broadly, these results also indicate that the biosynthetic pathways in the central
401 metabolism, e.g. amino acid biosynthesis, are the most important factors controlling $\delta^{13}C$
402 variability between individual amino acids. In comparison, isotope effects caused by metabolic
403 routing between major macromolecular groups appear to be less important. However, $\delta^{13}C$ values
404 of a few amino acids did correlate with amino acid composition. As noted above, from the
405 pyruvate family, Ala $\delta^{13}C$ values correlated with the molar composition of most amino acid families
406 ($R^2 = 0.60$). Isotope values of two amino acids from the shikimate family, Tyr and Phe, also had
407 similar correlations as Ala but with opposite relationships ($R^2 = 0.45$) Since pyruvate and shikimate
408 both uses phosphoenolpyruvate as a precursor, it is possible that part of the variability in $\delta^{13}C_{AA}$

patterns between different growth conditions can be explained by routing at branching points in the central metabolism.

Three remaining amino acids, Thr, Asx, and Arg had higher than average $\delta^{13}C$ variability (Fig. 3), but did not correlate to any of the environmental and physiological parameters tested. A previous study comparing $\delta^{13}C_{AA}$ values between leaf and seed protein amino acids, also found Thr and Asx to be the most variable of all the amino acids (Lynch et al., 2011). The authors suggested that these two amino acids may be synthesized within the seeds rather than transported from the leaves, potentially resulting in a different isotopic composition from that in leaves. A similar compartmentalization does not exist for the unicellular diatoms, except for storage of protein amino acids in vacuoles (see discussion below); however, one possibility is that the variability in Thr isotope values can be attributed to the carbon flux distributed between the biosynthesis of Lys and the biosynthesis of Met and Thr (Bromke, 2013). A two-way downstream flux also exists for oxaloacetate, the immediate precursor for Asx, as is the case for Ala. Finally, the high $\delta^{13}C_{AAnor}$ variability for Arg may be analytical in nature, attributable to typical high signal to noise ratios during isotope analysis.

Changes in amino acid composition could also be related to changes in the diatom's protein content and intracellular storage nitrogen pool. The fact that C : N ratios and cell size were correlated indicates that there is a preferential storage of certain amino acids in the diatom's intracellular storage pool. These pools (or vacuoles) contain mostly nitrate, and play an important role for cell division and dissimilatory nitrate reduction under dark and anoxic conditions (Kamp et al., 2013). Changes in molar amino acid composition can also be related to the diatoms' requirements for different amino acids under different growth conditions. Several studies have reported that diatoms change their protein content in response to higher temperatures, nutrient availability and salinity (Rousch et al., 2003; Araujo and Garcia, 2005; Diekmann et al., 2009). Given the large ecological role of marine diatoms, it is evident from such data that the high macromolecular plasticity of individual diatom species such as *T. weissflogii* has the potential to alter nutrient and energy fluxes in marine ecosystems (Sackett et al., 2013).

3.2 Sedimentary $\delta^{13}C_{AA}$ patterns

A central question for preservation of sedimentary OM (SOM) generally is the degree to which primary production source patterns are preserved, as opposed to microbially altered, during early diagenesis. We used heterotrophic bacteria as the microbial endmember because bacterial $\delta^{13}C_{AA}$ patterns are well established in contrast to those of archaea. Archaea are likely to play an important role for degradation in subsurface waters and sediments, but additional studies are needed for studying this topic in term of source diagnostic isotope patterns. In the first step of estimating the relative proportion of bacterial amino acids in sediments from the Peru Margin, we identified the amino acids that were most informative of diatom and bacterial origins using the $\delta^{13}C_{AA}$ fingerprinting method. As a training dataset we relied on a broad assemblage of laboratory cultured diatoms and bacteria. Larsen et al. (2009, 2013) have previously shown that heterotrophic bacterial $\delta^{13}C_{AA}$ patterns are broadly similar, and are clearly distinct from eukaryotic autotrophic sources. Hence, we used heterotrophic bacterial $\delta^{13}C_{AA}$ patterns as one endmember of our predictive classification model with time. We used diatoms as another source endmember, because of their importance as dominant primary producers in nutrient-rich upwelling environments world-wide. While the species assemblage of the ten diatom samples may not be

identical to the deposited algae at the sampling site, we contend that the laboratory cultured diatoms represent a reasonable $\delta^{13}C_{AA}$ endmember for coastal plankton sources since diatoms comprised between 50 and 80 % of the total algal remains in the sediment (Table 3). Previous $\delta^{13}C_{AA}$ work has indicated that $\delta^{13}C_{AA}$ patterns of different eukaryotic phytoplankton, especially diatoms, have relatively minor differences (Vokhshoori et al., 2014). Moreover, we demonstrated in the diatom culture experiment that $\delta^{13}C_{AA}$ patterns remain source diagnostics across varying environmental conditions. Therefore, we hypothesize that bacterial resynthesis of original algal production should clearly shift $\delta^{13}C_{AA}$ patterns, and so offer a novel approach for directly evaluating the importance of bacterial source in preserved SOM.

We explored two independent approaches for characterizing microbial contribution during sedimentary diagenesis; Bayesian mixing modeling with normalized $\delta^{13}C_{AA}$ values and pairwise $\delta^{13}C_{AA}$ differences. Results from both approaches showed that Ile, followed by Lys, Leu and Tyr were the most informative amino acids for distinguishing between bacterial algal sources, which is in good agreement with Larsen et al. (2013). It is particularly striking that the Bayesian model for directly estimating fraction of bacterial source (based on values of these four amino acids) showed essentially identical trends with time as $\delta^{13}C_{Lys\text{-}Leu}$ alone (Fig. 6). This similarity gives added confidence to the estimated bacterial fractions, despite the rather high uncertainties in estimated mean values (Table S4). These findings are encouraging in suggesting $\delta^{13}C_{AA}$ as a new, direct approach for quantifying microbial contribution to sedimentary organic matter, and in particular bacterially-derived organic nitrogen. However, further work is also clearly warranted, with higher resolution sampling, and in understanding how shifts in $\delta^{13}C_{AA}$ correspond with other more traditional proxies, including redox sensitive elements and diagenetic or bacterial markers such as D-amino acids and muramic acid (Grutters et al., 2002; Lomstein et al., 2009; Fernandes et al., 2014a). In terms of the methodological issues of analyzing sedimentary $\delta^{13}C_{AA}$, we found that purification did not alter $^{13}C_{AA}$ values except that Asx showed an enrichment of approximately 2 ‰. In our case, Asx was not informative of degradation processes and the 2 ‰ fractionation was therefore of no concern to this study. That said, it will be important to continue the method development of purifying complex samples to ensure that isotope effects are completely eliminated.

We did compare our results with the DI index, a commonly used degradation proxy based on molar amino acid composition (Dauwe and Middelburg, 1998; Dauwe et al., 1999). The finding of weak correlation between the DI index and the $\delta^{13}C_{AA}$ based proxy seem somewhat surprising. However, the range in DI values in this core is relatively modest, and there is no consistent trend of increasing DI index with sediment depth throughout the core (Table 3). This may be consistent with a low oxygen – high preservation environment, suggesting that DI index values could be related mainly to the sources and deposition of individual sediment horizons, as opposed to further change downcore. Ultimately, however, the apparent decoupling of these two parameters likely points to our currently limited mechanistic understanding of many commonly applied diagenetic parameters. The DI index is an operational parameter, developed based on multivariate analysis of changes in amino acid molar composition between different samples with a-priori assumed differences in degradation state (Duawe et. al., 1998). However, such molar changes could arise equally from selective degradation of autotrophic amino acids, or from addition of new bacterial biosynthate, or even from changes in amino acid pool that can be liberated by acid hydrolysis. The $\delta^{13}C_{AA}$ estimates of bacterial contribution, in contrast, reflect mostly essential amino acids synthesized by heterotrophic bacteria. Overall, coupling such parameters in future

work may offer major new opportunities to more fully understand mechanistic basis of sedimentary organic matter preservation. We also note that future research is needed in terms of understanding the resistance of proteinaceous sediment material to acid hydrolysis. To answer this question, it will be particularly important quantifying proteinaceous vs. non-proteinaceous fractions of organic nitrogen in the sediment (Keil et al., 2000). The single study to date directly comparing stable isotope values of bulk sedimentary nitrogen vs. the hydrolyzable proteinaceous amino acid pool suggests that the non-proteinaceous fraction of organic nitrogen is substantial (Batista et al, 2014).

It is also possible that degradation and resynthesis of amino acids in the water column could have shaped the $\delta^{13}C_{AA}$ patterns we observed in sediments. The proportion of amino acids degraded in the water column is usually large; for example, Lee and Cronin (1982) found that in the Peruvian upwelling region amino acid nitrogen declined from 75 to 90 % in fresh plankton to 10–30 % in the surface sediment. However, whether such degradation is predominantly due to amino acid removal, or if water column degradation also introduces significant bacterially-synthesized amino acids is not as clear. Lomstein et al. (2006) found for Chilean coastal upwelling areas that a large fraction of their measured D-amino acids in the sediment derived from diatom empty cell sacs and cell wall fragments, including peptidoglycan. The fact that these remains persisted in the sediment after cell death indicates that microbial degradation of diatom remains that reached the sea floor was relatively modest. Sinking particles caught in sediment traps usually have overall "fresh" biochemical signatures, relatively unaltered isotopic signatures (e.g. Cowie and Hedges, 1994; Hedges et al., 2001). Subsurface suspended POM, in contrast, often undergoes dramatic shifts in bulk N isotope signatures with depth consistent with microbial alteration (Zhang and Altabet, 2008), and also has typically older $\Delta^{14}C$ ages (Druffel et al., 1996). However, a recent paper examining $\delta^{13}C_{AA}$ in suspended POM (which had undergone an 8‰ shift in bulk isotope values with depth) did not find evidence that bacteria represented a significant source of organic material (Hannides et al., 2013). This finding is consistent with very low D/L amino acid ratios in similar particles (Kaiser and Benner, 2008). In sinking POM, the only compound specific isotope amino acid paper to date has found variable results. McCarthy et al. (2004) reported a strong imprint of heterotrophic resynthesis from surface waters in an equatorial upwelling region, corresponding with multiple other parameters indicating extensive heterotrophic organic matter alteration. In contrast, in an adjacent region sinking POM showed little change in $\delta^{13}C_{AA}$ patterns with depth, even in deep ocean (3600 m) traps. Overall, it seems possible that some portion of the surface sediment bacterial contributions can be attributed to processes during water column transit; however, not enough is known about $\delta^{15}N$ and $\delta^{13}C$ patterns in sinking particles to clearly constrain this possible source.

Taken together, these first sediment $\delta^{13}C_{AA}$ results indicate that even in relatively high deposition and low oxygen environment such as the Peru margin, microbial resynthesis has contributed substantially to amino acids preserved in oldest sediments. The correlation in our study between sediment age and bacterial amino acid contribution supports the idea of progressive accumulation of bacterial SOM, even in extremely well preserved sediments (Fig. 6). While the multivariate analysis showed that high total organic carbon content was also associated with less bacterial-like $\delta^{13}C_{AA}$ patterns (Table 4), the pairwise comparison between young and old layers with similar organic carbon content (e.g. 0.6 vs. 45.0 kyr, 5.2 vs. 43.3 kyr, Fig. 6) indicated that regardless of organic carbon content, bacterial SOM was more predominant in older layers. This observation supports the conclusion that sediment age, as opposed to organic carbon

content, is the most important driver of increasing bacterial contribution. It is possible that bacterial transformation could also have been linked to specific depositional conditions of specific sediment horizons (Grutters et al., 2002), but further cross-site studies are warranted to better understand what controls transformation from algal to bacterial derived SOM.

Conclusions and outlook

In this study we have presented a first assessment of the potential of $\delta^{13}C_{AA}$ patterns as new paleoproxies, first from the perspective of assessing the fidelity of $\delta^{13}C_{AA}$ sources in the face of variation in ocean growth conditions of primary producer sources, and second in terms of assessing possible post-depositional bacterial contributions to sedimentary organic matter. Our algal growth experiments have clearly demonstrated that, at least in one cosmopolitan marine species, $\delta^{13}C_{AA}$ patterns are good tracers of phylogenetic source, irrespective of wide variation in bulk isotope values, or biochemical cellular makeup linked to growth conditions. These results strongly support the potential to use now $\delta^{13}C_{AA}$ as a novel proxy for reconstructing detailed carbon sources and budgets in sediments, as well as potential in other paleoarchives. Finally, our results from sediments may be also be quite important for future studies of the role of bacteria in preservation of SOM, because they suggest that $\delta^{13}C_{AA}$ can also be used as a new tool to directly assess the extent of microbial contribution. Because amino acids are by far the most important form of preserved organic nitrogen in modern sediments, these data suggest that direct contribution of bacterially sourced biosynthetic to sedimentary organic nitrogen may be extensive.

Future research will need to explore in more detail the degree to which the extent of bacterial sedimentary amino acid resynthesis is linked to sedimentary regimes, and should also move to combine the information potential from both amino acid $\delta^{15}N$ and $\delta^{13}C$ values, in assessing the role of bacteria in sedimentary organic preservation. Specifically, these results pose a number of mechanistic questions, which we suggest should be important topics for future work. First, the results here are derived from the hydrolyzable amino acid pool, which is usually a fairly low proportion of total organic nitrogen in most sedimentary systems (e.g. Cowie and Hedges, 1994).

Since bacterial growth and resynthesis should, by definition, produce “fresh” proteinaceous material, it will be important to devise ways to understand if the trends in bacterial source indicated here are representative of the entire sediment amino acid pool, or rather mainly the “freshest” fraction, amenable to acid hydrolysis. Second, it will be important to determine if results indicating substantial bacterial source and resynthesis are general, or are specific to different sedimentary regimes. For example, Batista et al. (2014) recently examined $\delta^{15}N_{AA}$ patterns from laminated anoxic sediments in the Santa Barbara Basin. These authors found no evidence for bacterial modification in $\delta^{15}N_{AA}$ patterns past the sediment-water interface, a conclusion supported by $\delta^{15}N_{AA}$ based resynthesis parameters such as total heterotrophic amino acid resynthesis (ΣV) (McCarthy et al., 2007). While $\delta^{15}N_{AA}$ was not measured in this study, the apparent contrast between these two high productivity/deposition environments suggests that bacterial sources of resynthesized organic matter could be more variable than might initially be assumed. Finally, the apparent variability of bacterial contributions in this single core poses the fundamental question of what controlling mechanisms regulate percentage of post-deposition bacterial resynthesis. We suggest $\delta^{13}C_{AA}$ patterns can represent a key new tool for understanding

588 the direct role of bacterial resynthesis in SOM preservation.
589
590 ## Acknowledgement
591
592 The study was funded by the Deutsche Forschungsgemeinschaft, the Cluster of Excellence
593 "The Future Ocean" (EXC 80/1, CP0937); L. T. Bach was funded by the BMBF in the framework of
594 the BIOACID II project, M. Ventura was funded by the Spanish Government project Invasivefish
595 (427/2011). This work is a contribution to the DFG supported Sonderforschungsbereich 754
596 "Climate—Biogeochemistry interactions in the tropical ocean" (www.sfb754.de). We thank
597 Philippe Martinez and Elfi Mollier for providing the sediment samples.
598
599
600 ## References
601
602 [1] Amelung, W., and Zhang, X.: Determination of amino acid enantiomers in soils, Soil
603 Biology & Biochemistry, 33, 553-562, 10.1016/S0038-0717(00)00195-4, 2001.
604
605 [2] Araujo, S. D. and Garcia, V. M. T.: Growth and biochemical composition of the diatom
606 *Chaetoceros* cf. *wighamii* brightwell under different temperature, salinity and carbon dioxide
607 levels. I. Protein, carbohydrates and lipids, Aquaculture, 246, 405–412,
608 10.1016/j.aquaculture.2005.02.051, 2005.
609
610
611 [3] Arthur, K. E., Kelez, S., Larsen, T., Choy, C. A., and Popp, B. N.: Tracing the biosynthetic
612 source of essential amino acids in marine turtles using δ^{13}C fingerprints, Ecology, 95, 1285–1293,
613 10.1890/13-0263.1, 2014.
614
615
616 [4] Bach, L. T., Bauke, C., Meier, K. J. S., Riebesell, U., and Schulz, K. G.: Influence of
617 changing carbonate chemistry on morphology and weight of coccoliths formed by *Emiliania*
618 *huxleyi*, Biogeosciences, 9, 3449–3463, 10.5194/bg-9-3449-2012, 2012
619
620
621 [5] Batista, F. C., Ravelo, A. C., Crusius, J., Casso, M. A., and McCarthy, M. D.: Compound
622 specific amino acid δ^{15} N in marine sediments: A new approach for studies of the marine nitrogen
623 cycle, Geochim. Cosmochim. Ac., 142, 553–569, 10.1016/j.gca.2014.08.002, 2014.
624
625
626 [6] Bromke, M.: Amino Acid Biosynthesis Pathways in Diatoms, Metabolites, 3, 294–311,
627 2013.
628
629
630 [7] Burdige, D. J.: Preservation of organic matter in marine sediments: Controls,
631 mechanisms, and an imbalance in sediment organic carbon budgets?, Chem. Rev., 107, 467–485,
632 10.1021/cr050347q, 2007.

[8] Corr, L. T., Berstan, R., and Evershed, R. P.: Development of N-acetyl methyl ester derivatives for the determination of δ^{13}C values of amino acids using gas chromatography-combustion-isotope ratio mass spectrometry, Anal. Chem., 79, 9082–9090, 10.1021/ac071223b, 2007.

[9] Cowie, G. L. and Hedges, J. I.: Biochemical indicators of diagenetic alteration in natural organic matter mixtures, Nature, 369, 304–307, 10.1038/369304a0, 1994.

[10] Dauwe, B. and Middelburg, J. J.: Amino acids and hexosamines as indicators of organic matter degradation state in North Sea sediments, Limnol. Oceanogr., 43, 782–798, 10.4319/lo.1998.43.5.0782, 1998.

[11] Dauwe, B., Middelburg, J. J., Herman, P. M. J., and Heip, C. H. R.: Linking diagenetic alteration of amino acids and bulk organic matter reactivity, Limnol. Oceanogr., 44, 1809–1814, 10.4319/lo.1999.44.7.1809, 1999.

[12] Dickson, A. G., Sabine, C. L., and Christian, J. R.: Guide to best practices for ocean CO_2 measurements, PICES Special Publication, 191 pp., 2007.

[13] Diekmann, A. B. S., Peck, M. A., Holste, L., St John, M. A., and Campbell, R. W.: Variation in diatom biochemical composition during a simulated bloom and its effect on copepod production, J. Plankton Res., 31, 1391–1405, 10.1093/plankt/fbp073, 2009.

[14] Dohler, G. and Biermann, T.: Impact of UV-B radiation on the lipid and fatty acid composition of synchronized *Ditylum brightwellii* (West) Grunow, Z. Naturforschung C, 49, 607–614, 1994.

[15] Druffel, E. R. M., Bauer, J. E., Williams, P. M., Griffin, S., and Wolgast, D.: Seasonal variability of particulate organic radiocarbon in the northeast Pacific Ocean, J. Geophys. Res.-Oceans, 101, 20543–20552, 10.1029/96JC01850, 1996.

[16] Fernandes, L., Garg, A., and Borole, D. V.: Amino acid biogeochemistry and bacterial contribution to sediment organic matter along the western margin of the Bay of Bengal, Deep Sea Res. Part I, 83, 81–92, 10.1016/j.dsr.2013.09.006, 2014a.

[17] Fernandes, R., Millard, A. R., Brabec, M., Nadeau, M.-J., and Grootes, P.: Food Reconstruction Using Isotopic Transferred Signals (FRUITS): A Bayesian Model for Diet Reconstruction, Plos One, 9, e87436, 10.1371/journal.pone.0087436, 2014b.

[18] Field, C. B., Behrenfeld, M. J., Randerson, J. T., and Falkowski, P.: Primary production of the biosphere: Integrating terrestrial and oceanic components, Science, 281, 237–240, 10.1126/science.281.5374.237, 1998.

[19] Grootes, P. M., Nadeau, M.-J., and Rieck, A.: ^{14}C-AMS at the Leibniz-Labor: radiometric dating and isotope research, Nuclear Instrum. Method. Phys. Res. Sect. B: Beam Interactions with Materials and Atoms, 223–224, 55–61, 10.1016/j.nimb.2004.04.015, 2004.

[20] Grutters, M., van Raaphorst, W., Epping, E., Helder, W., de Leeuw, J. W., Glavin, D. P., and Bada, J.: Preservation of amino acids from in situ-produced bacterial cell wall peptidoglycans in northeastern Atlantic continental margin sediments, Limnol. Oceanogr., 47, 1521–1524, 10.4319/lo.2002.47.5.1521, 2002.

[21] Guillard, R. R. and Ryther, J. H.: Studies of marine planktonic diatoms. I. *Cyclotella nana* Hustedt, and *Detonula confervacea* (cleve) Gran, Canadian J. Microbiol., 8, 229–239, 1962.

[22] Hartnett, H. E., Keil, R. G., Hedges, J. I., and Devol, A. H.: Influence of oxygen exposure time on organic carbon preservation in continental margin sediments, Nature, 391, 572–574, 10.1038/35351, 1998.

[23] He, H. B., Lu, H. J., Zhang, W., Hou, S. M., and Zhang, X. D.: A liquid chromatographic/mass spectrometric method to evaluate ^{13}C and ^{15}N incorporation into soil amino acids, J Soil Sediment, 11, 731-740, DOI 10.1007/s11368-011-0360-5, 2011.

[24] Hedges, J. I. and Keil, R. G.: Sedimentary organic matter preservation: an assessment and speculative synthesis, Mar. Chem., 49, 81–115, 10.1016/0304-4203(95)00008-F, 1995.

[25] Hedges, J. I., Baldock, J. A., Gelinas, Y., Lee, C., Peterson, M., and Wakeham, S. G.: Evidence for non-selective preservation of organic matter in sinking marine particles, Nature, 409, 801–804, 10.1038/35057247, 2001.

[26] Henderson, G. M.: New oceanic proxies for paleoclimate, Earth Planet. Sc. Lett., 203,

1–13, 10.1016/S0012-821x(02)00809-9, 2002.

[27] Kaiser, K. and Benner, R.: Major bacterial contribution to the ocean reservoir of detrital organic carbon and nitrogen, Limnol. Oceanogr., 53, 99–112, 10.4319/lo.2008.53.1.0099, 2008.

[28] Kamp, A., Stief, P., Knappe, J., and de Beer, D.: Response of the Ubiquitous Pelagic Diatom *Thalassiosira weissflogii* to Darkness and Anoxia, Plos One, 8, e82605, 10.1371/journal.pone.0082605, 2013.

[29] Keil, R. G., Tsamakis, E., and Hedges, J. I.: Early diagenesis of particulate amino acids in marine systems, in: Perspectives in amino acid and protein geochemistry, edited by: Goodfriend, G. A., Collins, M. J., Fogel, M. L., Macko, S. A., and Wehmiller, J. F., Oxford University Press, Oxford ; New York, 69-82, 2000.

[30] Larsen, T., Ventura, M., Damgaard, C., Hobbie, E. A., and Krogh, P. H.: Nutrient allocations and metabolism in two collembolans with contrasting reproduction and growth strategies, Funct. Ecol., 23, 745–755, 10.1111/j.1365-2435.2009.01564.x, 2009.

[31] Larsen, T., Ventura, M., Andersen, N., O'Brien, D. M., Piatkowski, U., and McCarthy, M. D.: Tracing Carbon Sources through Aquatic and Terrestrial Food Webs Using Amino Acid Stable Isotope Fingerprinting, Plos One, 8, e73441, 10.1371/journal.pone.0073441, 2013.

[32] Lee, C. and Cronin, C.: The Vertical Flux of Particulate Organic Nitrogen in the Sea – Decomposition of Amino Acids in the Peru Upwelling Area and the Equatorial Atlantic, J. Mar. Res., 40, 227–251, 1982.

[33] Lee, C., Wakeham, S. G., and I. Hedges, J.: Composition and flux of particulate amino acids and chloropigments in equatorial Pacific seawater and sediments, Deep Sea Res. Part I, 47, 1535–1568, 10.1016/s0967-0637(99)00116-8, 2000.

[34] Lomstein, B. A., Jorgensen, B. B., Schubert, C. J., and Niggemann, J.: Amino acid biogeo- and stereochemistry in coastal Chilean sediments, Geochim. Cosmochim. Ac., 70, 2970–2989, 10.1016/j.gca.2006.03.015, 2006.

[35] Lomstein, B. A., Niggemann, J., Jørgensen, B. B., and Langerhuus, A. T.: Accumulation of prokaryotic remains during organic matter diagenesis in surface sediments off Peru, Limnol.

Oceanogr., 54, 1139–1151, 10.4319/lo.2009.54.4.1139, 2009.

[36] Lynch, A. H., McCullagh, J. S. O., and Hedges, R. E. M.: Liquid chromatography/isotope ratio mass spectrometry measurement of delta ^{13}C of amino acids in plant proteins, Rapid Commun. Mass Sp., 25, 2981–2988, 10.1002/rcm.5142, 2011.

[37] Makou, M. C., Eglinton, T. I., Oppo, D. W., and Hughen, K. A.: Postglacial changes in El Niño and La Niña behavior, Geology, 38, 43–46, 10.1130/G30366.1, 2010.

[38] McCarthy, M. D., Benner, R., Lee, C., Hedges, J. I., and Fogel, M. L.: Amino acid carbon isotopic fractionation patterns in oceanic dissolved organic matter: an unaltered photoautotrophic source for dissolved organic nitrogen in the ocean?, Mar. Chem., 92, 123–134, 10.1016/j.marchem.2004.06.021, 2004.

[39] McCarthy, M. D., Benner, R., Lee, C., and Fogel, M. L.: Amino acid nitrogen isotopic fractionation patterns as indicators of heterotrophy in plankton, particulate, and dissolved organic matter, Geochim. Cosmochim. Ac., 71, 4727–4744, 10.1016/j.gca.2007.06.061, 2007.

[40] Meyers, P. A.: Applications of organic geochemistry to paleolimnological reconstructions: a summary of examples from the Laurentian Great Lakes, Org. Geochem., 34, 261–289, 10.1016/S0146-6380(02)00168-7, 2003.

[41] Mollier-Vogel, E.: Peruvian Oxygen Minimum Zone Dynamics During the Last 18 000 Years, PhD dissertation from Mathematisch-Naturwissenschaftlichen Fakultät der Christian-Albrechts Universität zu Kiel, 2012.

[42] Nelson, D. M., Treguer, P., Brzezinski, M. A., Leynaert, A., and Queguiner, B.: Production and dissolution of biogenic silica in the ocean: Revised global estimates, comparison with regional data and relationship to biogenic sedimentation, Global Biogeochem. Cy., 9, 359–372, 10.1029/95gb01070, 1995.

[43] Nguyen, R. T. and Harvey, H. R.: Protein and amino acid cycling during phytoplankton decomposition in oxic and anoxic waters, Org. Geochem., 27, 115–128, 10.1016/S0146-6380(97)00076-4, 1997.

[44] Ortlieb, L., Vargas, G., and Saliege, J. F.: Marine radiocarbon reservoir effect along the

northern Chile-southern Peru coast (14–24 S) throughout the Holocene, Quaternary Res., 75, 91–103, 10.1016/j.yqres.2010.07.018, 2011.

[45] Reimer, P. J., Baillie, M. G. L., Bard, E., Bayliss, A., Beck, J. W., Blackwell, P. G., Ramsey, C. B., Buck, C. E., Burr, G. S., Edwards, R. L., Friedrich, M., Grootes, P. M., Guilderson, T. P., Hajdas, I., Heaton, T. J., Hogg, A. G., Hughen, K. A., Kaiser, K. F., Kromer, B., McCormac, F. G., Manning, S. W., Reimer, R. W., Richards, D. A., Southon, J. R., Talamo, S., Turney, C. S. M., van der Plicht, J., and Weyhenmeye, C. E.: Intcal09 and Marine09 Radiocarbon Age Calibration Curves, 0–50 000 Years Cal Bp, Radiocarbon, 51, 1111–1150, 2009.

[46] Rousch, J. M., Bingham, S. E., and Sommerfeld, M. R.: Changes in fatty acid profiles of thermo-intolerant and thermo-tolerant marine diatoms during temperature stress, J. Exp. Mar. Biol. Ecol., 295, 145–156, 10.1016/S0022-0981(03)00293-4, 2003.

[47] Sackett, O., Petrou, K., Reedy, B., De Grazia, A., Hill, R., Doblin, M., Beardall, J., Ralph, P., and Heraud, P.: Phenotypic Plasticity of Southern Ocean Diatoms: Key to Success in the Sea Ice Habitat?, Plos One, 8, e81185, 10.1371/journal.pone.0081185, 2013.

[48] Salvatteci, R., Field, D., Sifeddine, A., Ortlieb, L., Ferreira, V., Baumgartner, T., Caquineau, S., Velazco, F., Reyss, J.-L., Sanchez-Cabeza, J.-A., and Gutierrez, D.: Cross-stratigraphies from a seismically active mud lens off Peru indicate horizontal extensions of laminae, missing sequences, and a need for multiple cores for high resolution records, Mar. Geol., 357, 72–89, 10.1016/j.margeo.2014.07.008, 2014.

[49] Schönfeld, J., Kuhnt, W., Erdem, Z., Flögel, S., Glock, N., Aquit, M., Frank, M., and Holbourn, A.: Systematics of past changes in ocean ventilation: a comparison of Cretaceous Ocean Anoxic Event 2 and Pleistocene to Holocene Oxygen Minimum Zones, Biogeosciences Discuss., 11, 13343–13387, 10.5194/bgd-11-13343-2014, 2014.

[50] Skilbeck, C. G. and Fink, D.: Radiocarbon dating and sedimentation rates for Holocene – upper Pleistocene sediments, eastern equatorial Pacific and Peru continental margin, Data report ODP Leg-181, in: Proc. ODP, Sci. Results, 201, edited by: Jørgensen, B. B., D'Hondt, S. L., and Miller, D. J., 2006.

[51] Torstensson, A., Hedblom, M., Andersson, J., Andersson, M. X., and Wulff, A.: Synergism between elevated pCO_2 and temperature on the Antarctic sea ice diatom *Nitzschia lecointei*, Biogeosciences, 10, 6391–6401, 10.5194/bg-10-6391-2013, 2013.

[52] Tribovillard, N., Algeo, T. J., Lyons, T., and Riboulleau, A.: Trace metals as paleoredox and paleoproductivity proxies: An update, Chem. Geol., 232, 12–32, 10.1016/j.chemgeo.2006.02.012, 2006.

[53] Tsuzuki, M., Ohnuma, E., Sato, N., Takaku, T., and Kawaguchi, A.: Effects of CO_2 concentration during growth on fatty-acid composition in microalgae, Plant Physiol., 93, 851–856, 10.1104/Pp.93.3.851, 1990.

[54] Venables, W. N. and Ripley, B. D.: Modern applied statistics with S, 4th ed., Statistics and computing, Springer, New York, xi, 495 pp., 2002.

[55] Vokhshoori, N., Larsen, T., and McCarthy, M.: Reconstructing $\delta^{13}C$ isoscapes of phytoplankton production in a coastal upwelling system with amino acid isotope values of littoral mussels, Mar. Ecol.-Prog. Ser., 504, 59–72, 10.3354/meps10746, 2014.

[56] Wakeham, S. G., Lee, C., Hedges, J. I., Hernes, P. J., and Peterson, M. J.: Molecular indicators of diagenetic status in marine organic matter, Geochim. Cosmochim. Ac., 61, 5363–5369, 10.1016/s0016-7037(97)00312-8, 1997.

[57] Zhang, L. and Altabet, M. A.: Amino-group-specific natural abundance nitrogen isotope ratio analysis in amino acids, Rapid Commun. Mass Sp., 22, 559–566, 10.1002/Rcm.3393, 2008.

889 Table 1. Treatment description and growth parameters for the *Thalassiosira weissflogii* treatments.

Treatment	ID	Temp	Light	Light cycle	Salinity	pH at 17ºC	
		ºC	µmol m-2 s-1	D/L (h)	psu	Init.	Term
Control	Ctrl	17.0	120	12.00/12.00	30.2	8.08	8.35±0.00
Low pH	pH.L	17.0	120	12.00/12.00	30.2	7.65	8.15±0.01
High pH	pH.H	17.0	120	12.00/12.00	30.2	8.75	8.89±0.01
Low irradiance	Irr.L	17.0	50	12.00/12.00	30.2	8.08	8.36±0.06
High irradiance	Irr.H	17.0	490	12.00/12.00	30.2	8.08	8.40±0.04
Low salinity	Psu.L	17.0	100	12.00/12.00	12.3	7.99	8.60±0.05
18ºC	T.18	18.0	100	12.00/12.00	30.9	8.02	8.68±0.01
27ºC	T.27	27.0	100	12.00/12.00	30.9	7.90	8.55±0.04
UV filter outdoor	UV.ct	10.6[1]	715[2]	15.35/8.25	30.9	8.13	8.60±0.00
No UV filter outdoor	UV.tr	10.6[1]	715[2]	15.35/8.25	30.9	8.13	8.59±0.04

890 [1]Temperature and [2]irradiance values are means of outdoor conditions; the 25% and 75% quartiles for temperature were 9.8 and 11.3ºC,
891 and the 25% and 75% quartiles for irradiance levels were 269 and 1274 µmol m^{-2} s^{-1}.
892

Table 2. Growth rates, bulk isotope values, elemental composition (expressed as percentage by mass), and relative composition (mole based) of amino acids according to biosynthetic precursors for *Thalassiosira weissflogii* (mean±stdev, n=3). See Table 1 for treatment identities.

ID	Growth rate	Cell density	Cell size	Bulk isotopes		Elemental composition			Relative amino acid composition*				
	d^{-1}	Cells ml^{-1}	µm diam.	$\delta^{13}C$ (‰)	$\delta^{15}N$ (‰)	%C	%N	C:N (atomic)	Pyruvate (%)	Oxalo (%)	α-keto (%)	3-PGA (%)	Shikimate (%)
Ctrl	0.735±0.016	6560±773	12.6±0.2	-22.9±0.3	4.8±0.6	24.3±2.6	1.93±0.18	10.8±0.3	22.0±0.3	30.4±0.4	18.3±0.3	15.0±0.4	14.2±0.4
Irr.L	0.483±0.016	6283±1270	13.6±0.5	-22.5±0.4	2.4±0.6	23.3±2.3	2.42±0.19	8.3±1.3	22.3±1.2	30.7±0.3	19.5±0.6	13.9±1.0	13.6±0.7
Irr.H	0.769±0.010	8287±741	12.5±0.1	-23.2±0.3	3.4±0.2	23.1±0.7	1.97±0.08	10.1±0.2	21.1±2.7	30.1±0.6	18.7±0.5	15.6±1.2	14.5±0.8
pH.L	0.732±0.002	6865±90	12.9±0.1	-23.4±0.1	4.7±0.0	24.8±0.6	1.93±0.03	11.0±0.3	21.3±1.0	30.4±0.2	18.7±0.3	15.2±0.3	14.4±0.6
pH.H	0.721±0.008	6799±421	12.9±0.0	-19.1±0.3	4.0±0.5	20.1±1.3	1.59±0.28	10.7±0.2	20.3±0.0	29.9±0.2	18.2±0.2	16.7±0.3	14.8±0.0
Psu.L	0.946±0.022	15190±2467	15.3±0.0	-29.1±0.6	1.9±0.4	31.4±0.5	4.55±0.20	5.9±0.2	28.2±0.3	28.2±0.1	19.5±0.2	11.4±0.3	12.7±0.3
T.18	0.878±0.015	9388±924	14.4±0.4	-19.3±0.2	0.8±0.3	25.9±1.5	2.96±0.40	7.6±0.6	26.1±1.0	28.6±1.0	19.5±0.9	12.8±0.8	12.8±0.4
T.27	1.343±0.015	16962±1274	14.9±0.5	-18.3±0.4	-0.9±0.2	24.2±2.2	4.59±0.27	4.5±0.1	27.7±0.2	28.8±0.8	19.4±0.7	12.0±0.4	12.2±0.8
UV.ct	0.510±0.003	5501±156	14.4±0.3	-23.0±0.3	3.1±0.6	28.2±2.3	3.07±0.20	7.9±0.6	22.3±1.8	30.0±1.2	21.8±0.7	12.5±0.7	13.3±0.8
UV.tr	0.505±0.012	5248±665	14.6±0.1	-23.4±0.4	3.0±1.0	30.6±0.8	3.54±0.15	7.2±0.3	22.1±1.2	30.5±1.5	21.8±0.3	12.6±0.5	13.0±1.2

*Pyruvate: Ala, Leu, Val. Oxaloacetate: Asx, Ile, Lys, Met, Thr. α-ketoglutarate: Arg, Glx. 3-phosphoglycerate: Gly, Ser. Shikimate: Phe, Tyr.

Table 3. Characteristics of sediment core M772-003-2 with depth, estimated age, total nitrogen (TN), $\delta^{15}N$ values, organic carbon, alkenones, algal abundance and percentage of upwelling species (based on *Chaetoceros* resting spores, *Pseudo-nitzschia* spp, *Thalassionema nitzschioides*). The degradation index (DI) was calculated based on (Dauwe et al., 1999).

ID	Depth	Age	TN	$\delta^{15}N$	C_{org}	Alkenone conc.	Algal abundance	Upwelling species	DI
	cm	ka	%	‰	wt.%	ng g^{-1}	10^6 cm^{-3}	%	
sed8	8	0.47	0.74	5.9	5.56	10504	77.2	60.8	-0.47
sed13	13	0.60	0.46	6.6	4.11	7477	77.2	60.8	-0.28
sed268	268	4.29	0.41	8.5	5.82	2764	178.9	67.9	0.49
sed278	278	4.40	0.63	5.0	5.82	5077	208.1	81.0	-0.17
sed353	353	5.20	0.31	8.4	2.90	1322	213.2	79.4	0.82
sed638	638	8.96	0.52	6.8	5.07	5925	69.9	75.6	0.10
sed689	698	9.66	0.48	6.5	3.57	4492	39.5	70.3	0.82
sed998	998	16.96	0.26	9.23	2.41	4214	26.6	50.0	1.10
sed1023	1023	17.33	0.33	8.8	3.15	5360	92.3	71.7	0.11
sed1283	1283	44.29	0.31	6.4	3.32	6487	251.3	66.4	0.76
sed1413	1413	45.01	0.45	5.8	4.75	8744	145.0	72.5	0.31

Table 4. Linear regression tables with one or more explanatory variables that explain $\delta^{13}C_{AA}$ values from sediment core M772-003-2. We applied penalized log likelihood to simplify the model, and fitted main effects without interactions. Following explanatory variables were tested: sediment age (s.age), abundance (alg.abun), bulk $\delta^{15}N$, organic C content ($\%C_{org}$), %N (pr.N), C/N ratio, algal cell numbers and % upwelling species. To focus on the most important results we only display significant results with R-squared values greater than 50%. 'Regr. coef.' signifies regression coefficient, and 'stdev' signifies standard deviation. Non-significant regressions are not shown.

$\delta^{13}\mathbf{C}_{\mathbf{Lys\text{-}Leu}}$; $F_{3,7}$ = 84.4, R^2 = 0.973, P < 0.001

`Independent variable	Regr. coef.±stdev	t value	P	
Intercept	9.0±0.3	34.0	$4.9*10^{-9}$	***
sediment age	$-4.9*10^{-5}$±$4.6*10^{-6}$	-10.7	$1.4*10^{-5}$	***
$\%C_{org}$	0.38±0.06	6.6	$3.1*10^{-4}$	***
Algal abundance	$5.2*10^{-3}$±$9.2*10^{-4}$	5.6	$8.0*10^{-4}$	***

$\delta^{13}\mathbf{C}_{\mathbf{Ile\text{-}Leu}}$; $F_{2,8}$ = 11.7, R^2 = 0.745, P<0.01

Independent variable	Regr. coef.±stdev	t value	P	
Intercept	4.8±1.0	4.9	0.0012	**
sediment age	$-5.2*10^{-5}$±$1.6*10^{-5}$	-3.3	0.0113	*
$\%C_{org}$	0.51±0.21	2.5	0.0386	*

$\delta^{13}\mathbf{C}_{\mathbf{Tyr\text{-}Leu}}$; $F_{2,8}$ = 8.45, R^2 = 0.679, P<0.05

Independent variable	Regr. coef.±stdev	t value	P	
Intercept	2.4±0.80	3.0	0.0185	*
sediment age	$-3.4*10^{-5}$±$1.3*10^{-5}$	-2.6	0.0292	*
$\%C_{org}$	0.376±0.167	2.2	0.055	

$\delta^{13}\mathbf{C}_{\mathbf{Glx\text{-}Phe}}$; $F_{1,8}$ = 9.48, R^2 = 0.542, P<0.05

Independent variable	Regr. coef.±stdev	t value	P	
Intercept	-5.41±0.45	-11.9	$2.30*10^{-6}$	***
%N	-2.91±0.94	-3.1	0.0151	*

Figure 1: Average $\delta^{13}C_{AA}$ and $\delta^{13}C_{bulk}$ values (n = 3) of *Thalassiosira weissflogii* across ten treatments (Tr.ID). See Table 1 for treatment descriptions and Table S1 for standard deviation values.

Figure 2: Distribution of relative differences in individual $\delta^{13}C_{AA}$ and $\delta^{13}C_{bulk}$ values of *Thalassiosira weissflogii* (28 samples) across ten different treatments. The "non-normalized" boxplots represent absolute differences in $\delta^{13}C$ values (as shown in Fig. 1) and the "normalized" boxplots represent differences for $\delta^{13}C$ values normalized to the amino acid mean for each treatment. The upper and lower whiskers indicate maximum and minimum values, the boxes show the 25th and 75th percentile range, and the line inside the boxes shows the median. The small dots show outlier values, and the large dots average values.

Figure 3: $\delta^{13}C_{AAnor}$ values of ten treatments relative to the control treatment (Ctrl; vertical broken line) for *Thalassiosira weissflogii* (the symbols and the horizontal bars represent the means and standard deviations including analytical errors). Different letters to the right of each figure indicate significant differences between treatments at $\leq$ 5 % significance levels (one-way ANOVA); the "-" symbol signifies that the given sample was omitted from the test due to missing replicates. See Table 1 for description of treatments.

Figure 4: Principal component analysis of $\delta^{13}C_{AAnor}$ values of giant kelp (*Macrocystis pyrifera*), seagrass (*Posidonia oceanica*) and diatoms (*Thalassiosira weissflogii*) showing that variation in $\delta^{13}C_{AA}$ pattern induced by varying growth conditions does not alter diagnostic tracer information. The two first axes accounting for 80 % of the variation separated the three marine taxa into distinct groups. All amino acids were important for the variations displayed by the two first ordination components. Thr was omitted owing to its large intraspecies variability.

Figure 5: A linear function discriminant analysis based on $\delta^{13}C_{AA}$ values identifying which set of amino acids that best distinguishes between diatoms (filled squares) and bacteria (filled circles). The two categorical variables are used to predict group membership of amino acids derived from sediment core M772-003-2 (open circles). The coefficients for each independent variable (crosses) are shown to the right; amino acids with the greatest absolute values are the most informative, i.e. Leu, Ile, Lys and Tyr. Amino acid abbreviations are as defined in text.

Figure 6: Estimated proportions of bacterial amino acids across sediment depths of core M772-003-2 using laboratory grown diatoms and bacteria as endmembers **(b)** compared to $\delta^{13}C_{Lys\text{-}Leu}$ values **(c)** and organic carbon content **(a)**. The Bayesian mixing modeling based on $\delta^{13}C$ values of Leu, Lys, Ile and Tyr **(b)** and pairwise differences between Lys and Leu, show a similar trend of increasing values as a funtion of sediment depth (or age). While organic carbon content can explain some of the co-variation of $\delta^{13}C_{Lys\text{-}Leu}$ (Table 4), sediment depth is the most influencial parameter for explaining the increasing values.

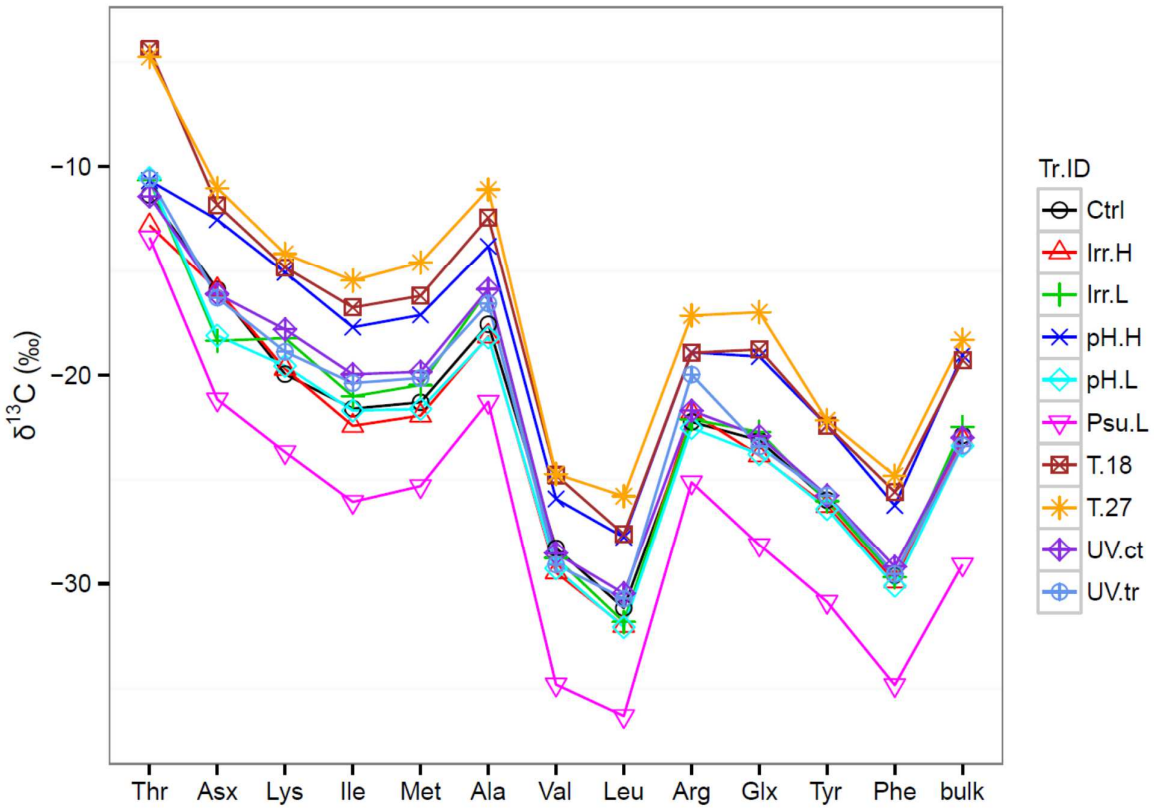

961
962 Figure 1
963

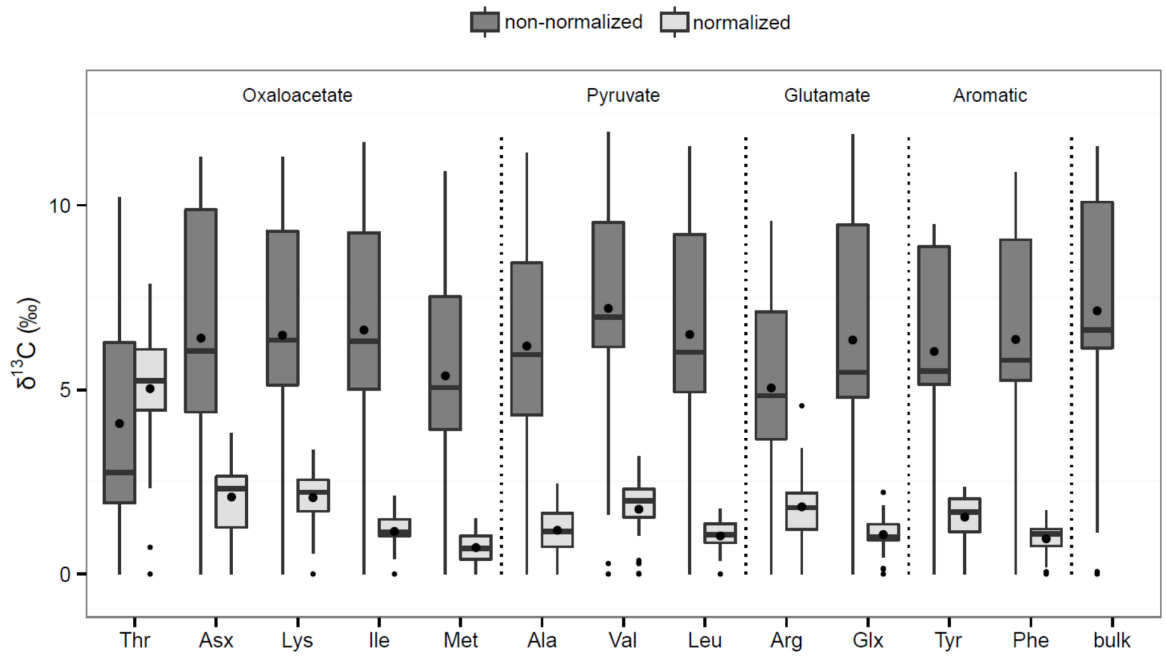
non-normalized
normalized
Oxaloacetate
Pyruvate
Glutamate
Aromatic
δ13C (‰)
10
5
0
Thr
Asx
Lys
Ile
Met
Ala
Val
Leu
Arg
Glx
Tyr
Phe
bulk

Figure 2

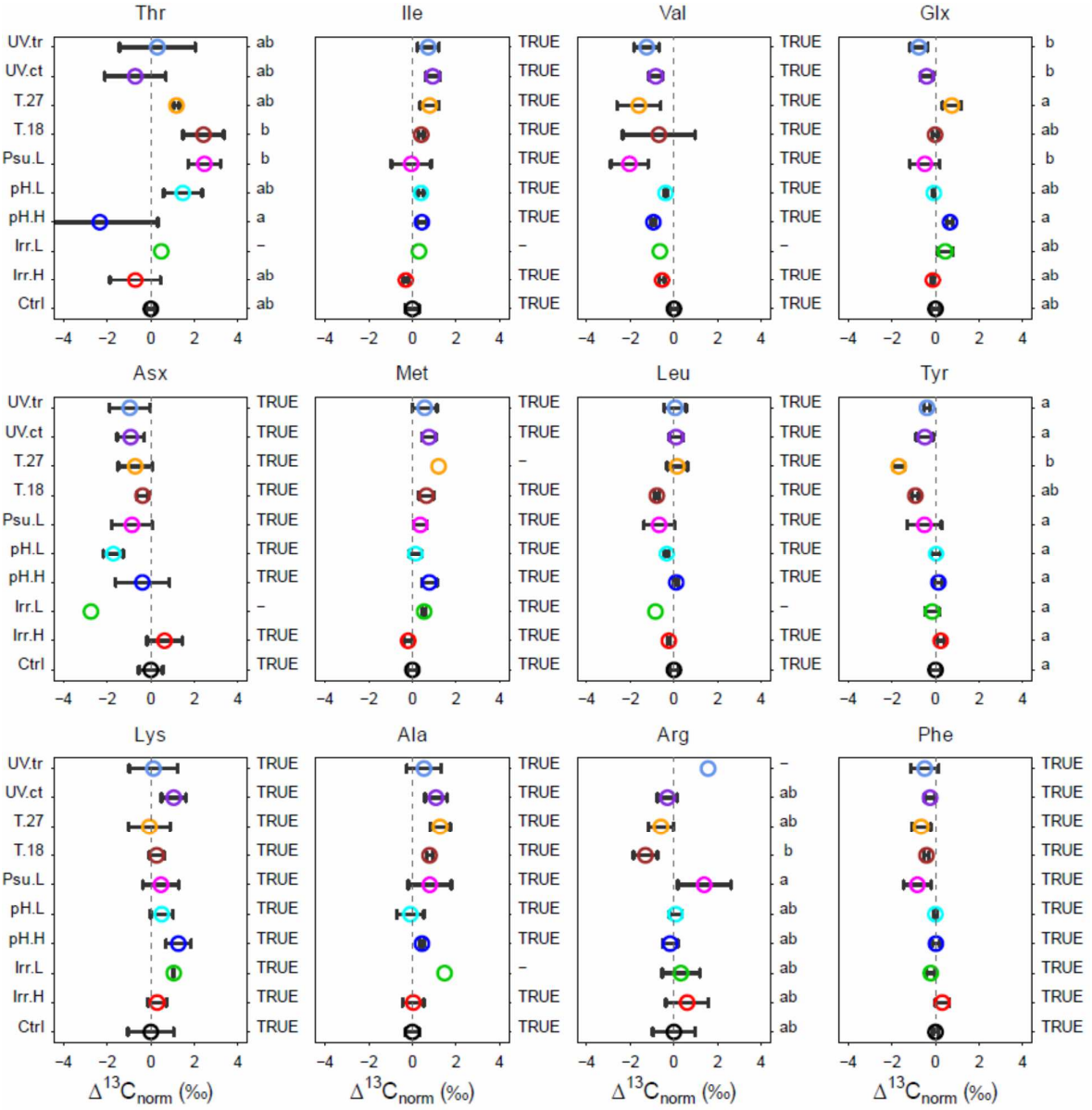
Thr
Ile
Val
Glx
Asx
Met
Leu
Tyr
Lys
Ala
Arg
Phe
UV.tr
UV.ct
T.27
T.18
Psu.L
pH.L
pH.H
Irr.L
Irr.H
Ctrl
−4 −2 0 2 4
Δ13Cnorm (‰)

Figure 3

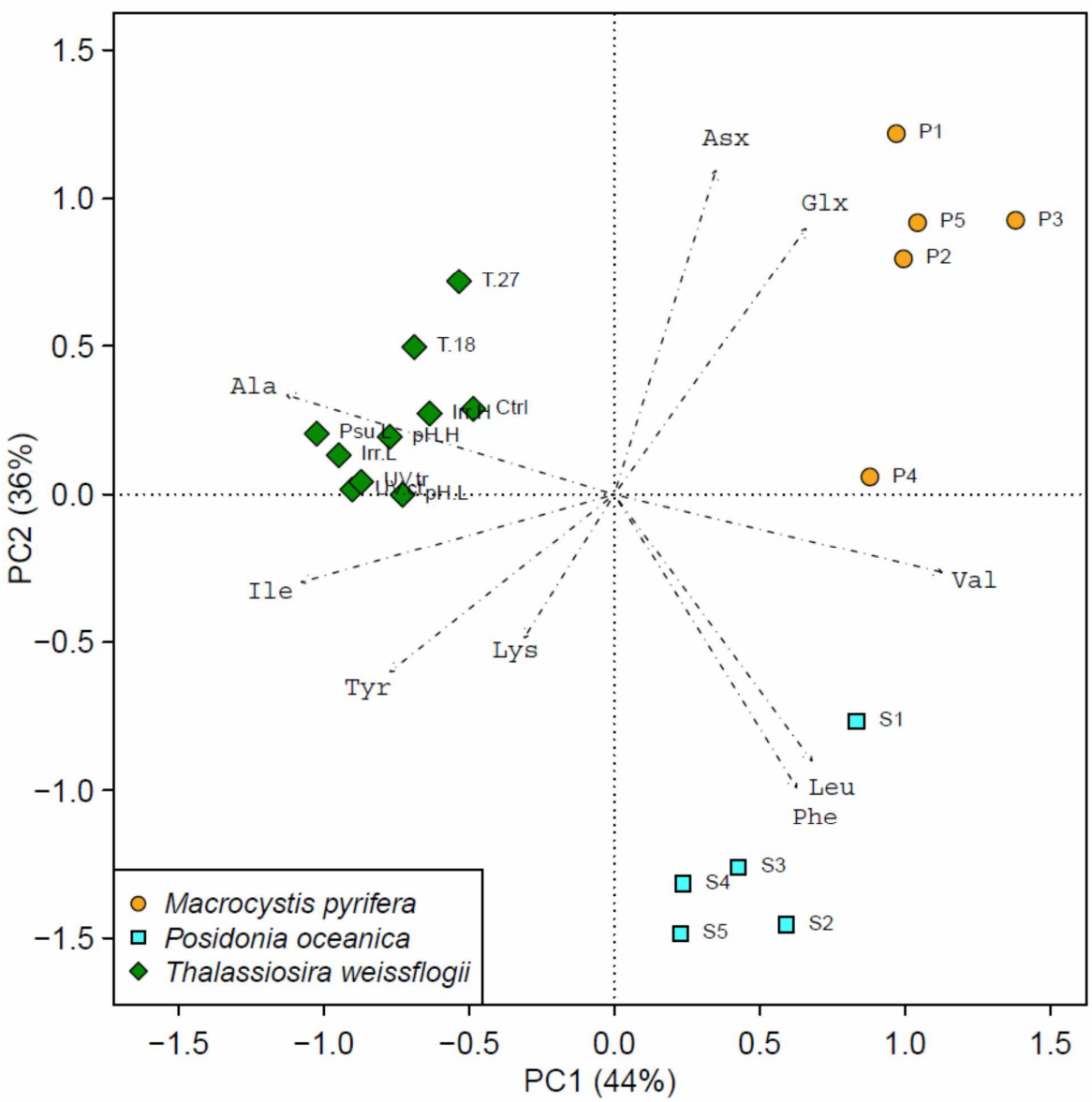
Asx
Glx
Ala
Ile
Lys
Tyr
Val
Leu
Phe
P1
P2
P3
P4
P5
S1
S2
S3
S4
S5
T.27
T.18
Ctrl
pH.H
pH.L
Irr.L
UV.tr
Macrocystis pyrifera
Posidonia oceanica
Thalassiosira weissflogii
PC1 (44%)
PC2 (36%)
1.5
1.0
0.5
0.0
−0.5
−1.0
−1.5

Figure 4

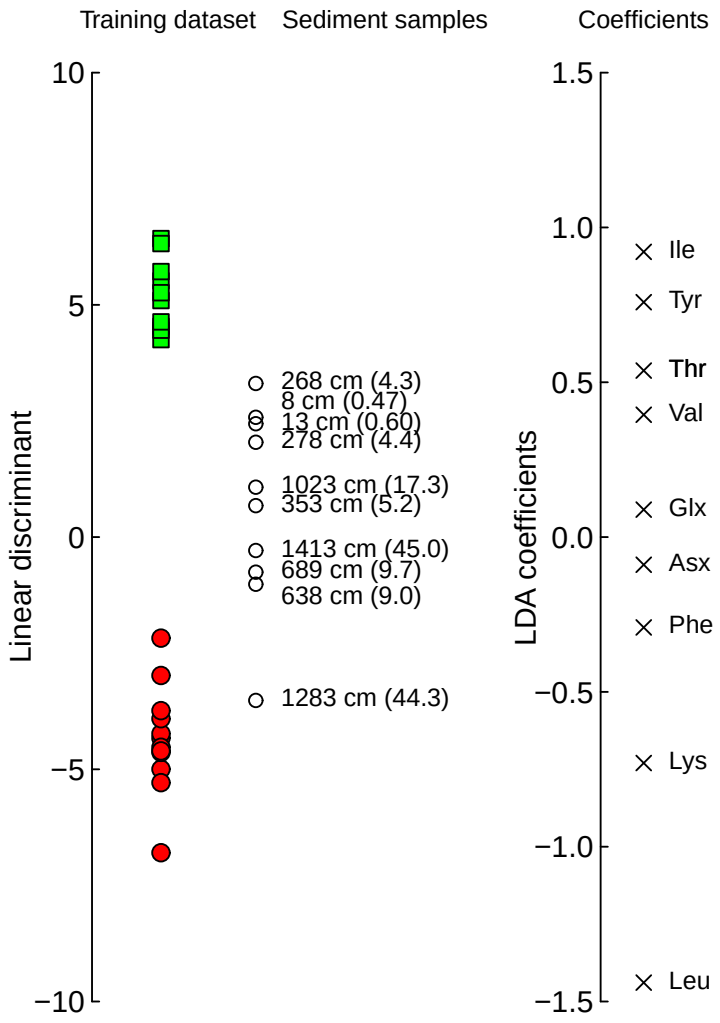

973
974 Figure 5
975

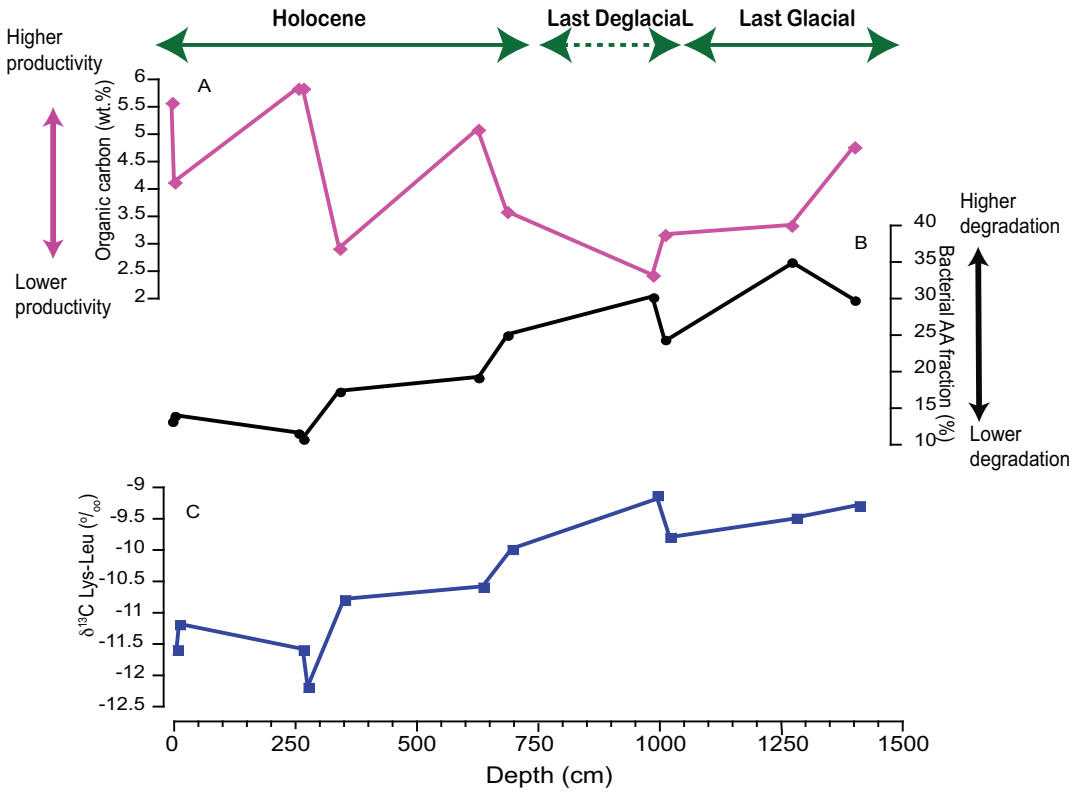
Holocene
Last DeglaciaL
Last Glacial
Higher productivity
Lower productivity
A
Organic carbon (wt.%)
B
Bacterial AA fraction (%)
Higher degradation
Lower degradation
C
δ13C Lys-Leu (‰)
Depth (cm)

Figure 6